Hybrid Active-and-Passive Relay Network Optimization of mmWave Communications for Industrial Internet

Zejing Yang[1], Jianzheng Wang[2], Yifeng Zhao[2*], Lianfen Huang[2], Zhiyuan Shi[1]

[1] Department of Electronic Science and Engineering, Xiamen University, China
[2] Department of Information and Communication Engineering and Key Laboratory of Digital Fujian on IoT Communication, Architecture and Security Technology (IoTCAS), Xiamen University, China
zejingyang@stu.xmu.edu.cn, JianzhengWang@stu.xmu.edu.cn, zhaoyf@xmu.edu.cn, lfhuang@xmu.edu.cn, zyshi@xmu.edu.cn

Abstract

Multi-hop relay selection is regarded as a key technology to overcome severe path loss and adapt complex environments in millimeter-wave (mmWave) and terahertz communication. Meanwhile, new hardware called reconfigurable intelligent surface (RIS) has emerged and is used to boost the spectral and energy efficiency of future wireless communication systems. Then, to solve the challenge that the numerous energy consumption caused by the increasing number of relays in the future industrial internet a promising architecture with a hybrid active–and-passive relay network is proposed in this paper. Then, the optimization joint system delay and energy efficiency based on the simulated annealing (SA) algorithm is considered in this paper. A hierarchical heuristic optimization algorithm with lower complexity is proposed and proved to be feasible under good communication conditions compared with other algorithms. Finally, numerical results demonstrate that the proposed hybrid relay system and joint optimization model can improve the energy efficiency of the network and reduce the system delay.

Keywords: Reconfigurable intelligent surface, Millimeter wave communication, Multi-hop hybrid relay selection, Joint optimization

1 Introduction

MmWave communication has raised enormous concern as a solution to the shortage of spectrum resources in the future and it is a great advantage of millimeter-wave communication to form narrow beams and reduce interference by using large-scale multi-input and multi-output (MIMO) technology. However, it comes with a set of challenges such as severe propagation loss and link blockages [1-2]. Besides, relaying is considered as one promising approach to resist blockage and improve coverage. Then, the ultra-dense relay network has been investigated spontaneously, which can solve the above problems and enhance the reliability and coverage of the communication link. Meanwhile, the ultra-dense relay network aroused a challenge that how to choose the best relay link in a complex scene. Two-hop relay selection is considered to improve the achievable rate in [3-4] and a mmWave multi-hop communications are considered to optimize the system throughput in [5-6]. However, energy efficiency is seldom considered in most literature about relay selection.

It's worth noting that, along with the number of relays increasing rapidly, energy consumption becomes a clamant problem. There are over 50 billion wireless capability devices anticipated to connect networks by 2020 [7] through dense deployments of numbers of access points [8-10]. Besides, a serious sustainability problem is posed for the future cellular networks, which requires 1000 times data rate compared with the current network and halve the energy consumption [11]. Moreover, although communication quality is enhanced significantly by the MIMO, mmWave, ultra-dense network (UDN) technologies, serious energy consumption problems are also introduced. Therefore, it is a challenge that how to improve system energy efficiency for achieving sustainable capacity growth in the future, while enhancing network performance. Recently, green communication has received huge interest in the research community [12-13]. Therein, the latest hardware technology emerges with the potential to significantly reduce energy consumption, which is the so-called RIS or Intelligent Reflecting Surface (IRS) [14-15].

RIS is a meta-surface equipped with integrated electronic circuits that can be programmed to alter an incoming electromagnetic field in a customizable way [16]. Moreover, owing to the passive structure, the power consumption is extremely low, and there is nearly no additional thermal noise added during reflecting. With densely deploying IRS in wireless networks and skillfully coordinating its reflection, the signal propagation or wireless channel between transmitter and receiver can be flexibly reconfigured to achieve the desired distribution or implementation, which provides a new method to fundamentally solve the problems of wireless channel fading damage and interference, and it is possible to realize the quantum leap improvement of wireless communication capacity and reliability [17]. Furthermore, light weight, low profile and low cost are part of the significant advantages of RIS, which means it can be easily installed on or removed from environment objects. Hence, it is a promising way to deploy a large number of RISs for relaying.

A great number of researches has been published recently in this area. A practical IRS phase shift model is proposed in [18], and the system performance is optimized by IRS assisted communication. In [20], deep reinforcement learning (DRL) is applied to improve the network throughput based on IRS-

*Corresponding Author: Yifeng Zhao; E-mail: zhaoyf@xmu.edu.cn
DOI: 10.53106/160792642022052303003

assisted communication. However, RIS-aided communication is based on the case that the transmitter and receiver are LOS transmission and Non-Line-of-Sight (NLOS) transmission is considered between the transmitter and receiver in few literatures, which is a common thing in millimeter-wave communication.

In some researches on IRS-supported transmission, [21] compares the classical repeat coded DF relay with IRS and numerical results show that the IRS requires hundreds of reconfigurable elements (each size of the antenna) to be competitive, even if an ideal phase shifted and frequency flat channel is considered. Besides, in [22], the potential applications of RISs in wireless networks are discussed, which operate at high-frequency bands, e.g., millimeter wave (30-100 GHz) and sub-millimeter wave (greater than 100 GHz) frequencies. Therein, numerical results are illustrated that higher the spectral efficiency gains of RISs when their size is sufficiently large as compared with the wavelength of the radio waves. Furthermore, A RIS-based downlink multiuser multiple input single-output (MISO) system is considered in [16] and numerical results are revealed obviously that the RIS-based communication can provide up to 300% higher energy efficiency (EE) than the active relay. Moreover, it was also confirmed that system EE depends on the number of mobile users and RIS components, as well as the single power consumption of RIS components.

It should be noted that, since RIS is a passive relay, it cannot provide sufficient gain for signal transmission to be demodulated and communicated by the receiver normally. Therefore, the hybrid active-and-passive relay network is a promising solution to the above problem. [23-24] considered a hybrid system of RIS auxiliary communication and active relay, but as mentioned earlier, NLOS communication is more common in the industrial Internet scenario, which is difficult to apply RIS auxiliary communication and cannot meet the requirements of mmWave communication.

In this paper, the hybrid active–and-passive relay network is investigated. We proposed a SA-based multi-hop hybrid relay selection strategy in mmWave communication. Furthermore, a hierarchical relay selection algorithm based on the greedy strategy with lower complexity is developed. Therein, RIS is considered as the passive relay and a finite number of reflecting units are equipped on the reconfigurable intelligent surface. The main contributions of this paper are listed as follows:

- A hybrid active and passive relay network is proposed, which is composed by AF relay and RIS. With it, the numerous energy consumption in mmWave communication can be greatly improved. Besides, considering that the uniform planar array (UPA) is used by RIS, we adopt a three-dimensional environment. The influence of outage probability caused by the obstruction is also considered in relay selection.
- A multi-hop relay selection model is developed, by which all possible number of hops are included to maximize the system performance.
- Considering the diversity of industrial Internet scenarios, a joint optimization model on system delay and energy efficiency is developed, which is more in line with the needs of different scenarios.
- The simulated annealing algorithm is presented to solve the complex optimization problem and hierarchical heuristic optimization is developed on the basis of greedy strategy, which has lower complexity. Finally, numerical results have been evaluated, which compare the performance of the SA-based algorithms with the exhaustive and greedy-based schemes.

The remainder of this paper is organized as follows. In Section II system model is introduced including the network model, signal model and the problem formulation. The SA-based and greedy-based joint optimization scheme is proposed in Section III and extensive numerically results are provided in Section IV. Finally, Section V makes a conclusion of the paper.

The notations used in this paper are listed as follows. $\mathcal{CN}(\mu,\sigma^2)$ denotes the circularly symmetric complex Gaussian (CSCG) distribution. $diag(x)$ denotes a diagonal matrix with each diagonal element being the corresponding element in x. $arg(x)$ denotes the principal value of the divergence angle of x. $|x|$ denotes the absolute value of a complex number x . For any vector ω (all vectors in this paper are column vectors), ω^H denote the conjugate transpose of. $Pr(P=1)$ denotes that the possibility of $P=1$.

2 System Model

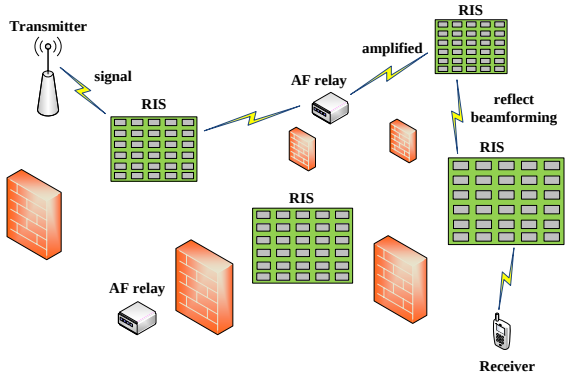

Figure 1. System model

2.1 Network Model

As shown in Figure 1, we consider a system model consists of a multi-hop hybrid AF relay and RIS network composed of source (S), relay (R), and destination (D). In addition, for a two-hop hybrid network, it is a half-duplex

sub-channel based on S-R-D, and for a three-hop hybrid network, it is based on three half-duplex sub-channels S-Rx-Ry-D. The higher hops can be obtained by analogy. Besides, it is assumed that the direct link between the source and the destination is interrupted and the same random characteristics are assumed in each time slot.

A factory is considered with an area of *s* and a height of *h*, where there is a source node, abundant relay nodes, a destination node, which relay nodes contain RISs and AF relays. The serviceable range *A* of each relay node is equal. It is assumed that each relay and RIS are consistent. The channel can be generated by the Saleh-Valenzuela (SV) channel model [25-28], which can be described as:

$$\boldsymbol{H} = \sqrt{\frac{N_t N_r}{L}} \sum_{l=0}^{L} \alpha_l \, \boldsymbol{a}_{r,l}(\varphi_{r,l}, \theta_{r,l}) \boldsymbol{a}_{t,l}^{H}(\varphi_{t,l}, \theta_{t,l}) \quad (1)$$

Denote N_t, N_r as the number of antennas equipped in the transmitters and receiving terminals respectively, α_l and L denotes gain of the path and the number of rays, which the number of clusters is not considered in the paper for simplification, $\boldsymbol{a}_{r,l}, \boldsymbol{a}_{t,l}$ respectively represents the array response vector at the receiving terminals and transmitters. Besides, considering the environment is usually complex and changeable, here obstacles are assumed randomly placed in the environment and we use the outage probability to represent it. Due to the poor penetration of millimeter waves, the outage probability is set to a random number ε_{RU} between each relay node and destination node, ε_R between relay nodes respectively, which can be expressed as:

$$\varepsilon_{RU} = Pr(P_{\text{out}} = 1) \quad (2)$$

$$\varepsilon_R = Pr(P_{\text{out}} = 1) \quad (3)$$

where, $\varepsilon_{RU} = \varepsilon_R + \varepsilon$, and ε is a constant, which reflects the complexity between each relay nodes and destination node in the scene and P_{out} represents whether the link is interrupted. If $P_{\text{out}} = 1$, it means that the selected link is blocked, then it will not be selected. In the factory scenario, the communication between relays is generally in LOS, while among the relay, receiver and transmitter, the communication is generally in NLOS. Therefore, the interrupt probability ε_{RU} will be greater than ε_R and the specific value depends on the environment.

2.2 Signal Model

A signal is considered as transmitted from the base station, and received by AF relay, which is given by:

$$y_{R_{AF}} = \sqrt{P_s} \boldsymbol{w_R} \boldsymbol{h}_{\boldsymbol{SR_{AF}}} \boldsymbol{f_S} s + n + n_r \quad (4)$$

where P_s is the base station transmit power, $\boldsymbol{w_R}$ is the received beam vector at AF relay, $\boldsymbol{h}_{\boldsymbol{SR_{AF}}}$ is the channel between the source node and AF relay, $\boldsymbol{f_S}$ is the transmitted beam vector at source node, s is the transmitted signal and $n \sim \mathcal{CN}(0, N_0)$, $n_r \sim \mathcal{CN}(0, N_1)$ are the background noise and receive noise at AF relay nodes.

Or received by RIS, which is given by:

$$y_{R_{RIS}} = \sqrt{P_S} \boldsymbol{h}_{\boldsymbol{SR_{RIS}}} \boldsymbol{\Phi} \boldsymbol{f_S} s + n \quad (5)$$

where $\boldsymbol{h}_{\boldsymbol{SR_{RIS}}}$ is the channel between the source node and RIS, $\boldsymbol{\Phi} = diag(\eta_1 e^{j\theta_1}, \ldots, \eta_N e^{j\theta_N})$, $\eta_i \in [0,1]$ $\theta_i \in [0, 2\pi]$ and n_r can be omitted because RIS does not introduce noise.

To simplify the analysis, it is assumed that there is ideal passive beamforming (IPB) with perfect channel estimation (PCE) at the RIS, and all elements have the same reflection amplitude. Hence, the phase and amplitude can be expressed as [19]:

$$\theta_i = -arg\left(\left[\boldsymbol{h}_{\boldsymbol{SR_{RIS}}} \right]_i \left[\boldsymbol{h}_{\boldsymbol{R_{RIS}D}} \right]_i \right) \eta_i = \eta, \forall i \quad (6)$$

where $\boldsymbol{h}_{\boldsymbol{R_{RIS}D}}$ is the channel between the RIS and destination node; then, the signal transmitted by the AF relay is:

$$y'_{R_{AF}} = \sqrt{P_r} \boldsymbol{f_R} y_{R_{AF}} \quad (7)$$

Or by the RIS, then is:

$$y'_{R_{RIS}} = y_{R_{RIS}} \quad (8)$$

where P_r is the transmit power of AF relay and $\boldsymbol{f_R}$ is the transmitted beam vector at AF relay.

Here, a two-hop relay communication is considered, the signal received by the target node can be expressed by:

$$y_D = \sqrt{P_S} \boldsymbol{w_D} \boldsymbol{h_{RD}} \boldsymbol{H_t} \boldsymbol{H_r} \boldsymbol{f_S} s + n_r + n \quad (9)$$

where $\boldsymbol{H_t}$, $\boldsymbol{H_r}$ can be expressed as:

$$\boldsymbol{H_t} = \begin{cases} \sqrt{P_r} \boldsymbol{f_R} & \text{relay is AF relay} \\ 1 & \text{relay is RIS} \end{cases} \quad (10)$$

$$\boldsymbol{H_r} = \begin{cases} \boldsymbol{w_R h} & \text{relay is AF relay} \\ \boldsymbol{h \Phi} & \text{relay is RIS} \end{cases} \quad (11)$$

where $\boldsymbol{w_D}$ is the received beam vector at destination node, $\boldsymbol{h_{RD}}$ is the channel between the last relay in a selected relay link and destination node, $\boldsymbol{w_R}$ is the received beam vector at AF relay, $\boldsymbol{h}$ is the channel between two adjacent relays in a selected relay link.

By analogy, a multi-hop hybrid relay network model is formulated, and the signal received by the user is given by:

$$y_D = \sqrt{P_S} \boldsymbol{w_D} \boldsymbol{h_{RD}} \prod_{i}^{i \in \mathcal{R}} (R(i) \boldsymbol{H_t} \boldsymbol{H_r}) \boldsymbol{f_S} s + n_r + n \quad (12)$$

where $\mathcal{R}$ represents all the relays in scene and $R(i)$ is the mark of relay selection, which indicate whether the relay is selected.

2.3 Problem Model

According above, the SNR at AF relay R_{AF_i} is given by:

$$\gamma_i = \frac{\left| \sqrt{P_S} \boldsymbol{w_R} \boldsymbol{h_R} \prod_i^{i \in \mathcal{R}'} (\boldsymbol{H_t} \boldsymbol{H_r}) \boldsymbol{f_S} \right|^2}{\left| \sqrt{P_S} \boldsymbol{w_R} \boldsymbol{h_R} \prod_i^{i \in \mathcal{R}'} (\boldsymbol{H_t} \boldsymbol{H_r}) \boldsymbol{f_S} \right|^2 + N_0^2 + N_1^2} \quad (13)$$

where $\mathcal{R}'$ represents the relays in a selected relay link.

Or at RIS R_{RIS_i} is given by:

$$\gamma_i = \frac{\left| \sqrt{P_S} \boldsymbol{h_R} \boldsymbol{\Phi} \prod_i^{i \in \mathcal{R}'} (\boldsymbol{H_t} \boldsymbol{H_r}) \boldsymbol{f_S} \right|^2}{\left| \sqrt{P_S} \boldsymbol{h_R} \boldsymbol{\Phi} \prod_i^{i \in \mathcal{R}'} (\boldsymbol{H_t} \boldsymbol{H_r}) \boldsymbol{f_S} \right|^2 + N_0^2} \quad (14)$$

Then, the SNR at destination node can be expressed as:

$$\gamma = \frac{\left|\sqrt{P_S}\boldsymbol{w_D}\boldsymbol{h_R}\prod_i^{i\in\mathcal{R}}(R(i)\,\boldsymbol{H_t}\boldsymbol{H_r})\boldsymbol{f_s}\right|^2}{\left|\sqrt{P_S}\boldsymbol{w_D}\boldsymbol{h_R}\prod_i^{i\in\mathcal{R}}(R(i)\,\boldsymbol{H_t}\boldsymbol{H_r})\boldsymbol{f_s}\right|^2 + N_0^2 + N_1^2} \quad \textbf{(15)}$$

Therefore, the achievable rate at relay R_i can be express as:

$$C_i = \frac{W}{2} log_2(1+\gamma_i) \quad \textbf{(16)}$$

where W is the communication bandwidth.

Hence, the capacity in the system can be express as:

$$C = min\{C_i, C_D\} \quad \textbf{(17)}$$

where C_D is the achievable rate at destination node.

Then, the spectrum effectiveness (SE) in the system can be given by:

$$\curlyvee = \frac{C}{W} \quad \textbf{(18)}$$

In addition, delay impact τ caused by relay is also considered, which can be expressed as:

$$\tau = \tau_{path} + \tau_{relay} \quad \textbf{(19)}$$

where τ_{path} is the delay of communication path, τ_{relay} is the delay generated by the AF relay node and RIS. The delay introduced by AF relay is τ_{AF} and the delay caused by RIS is τ_{RIS}.τ_{path} is given by:

$$\tau_{path} = \frac{\delta}{C} \quad \textbf{(20)}$$

where δ is transmission data size.

In the factory scenario, there are many automatic control devices that are sensitive to system delay, so it is a key communication index for the factory. Furthermore, we also take the energy efficiency (EE) into consideration and the energy efficiency η is given by:

$$\eta = \frac{C}{P_{all}} \quad \textbf{(21)}$$

where P_{all} represents the total power consumption of the communication system. It is obvious to observe that, the noise amplification effect is introduced at AF relay due to its unique characteristics. To simplify it, the amplification efficiency of the AF relay is used to represent its impact. Besides, as already described above, unlike RIS, RF power is needed to be consumed for the AF relay to amplify the received signal and transmit it. Therefore, P_{all} can be expressed as [16]:

$$P_{all} = \alpha * \xi P_r + P_S + (2 * \alpha N_{AF} + \beta N_{RIS})P_R \quad \textbf{(22)}$$

where ξdepends on the efficiency of the relay power amplifier, α , β is the number of selected AF relay and RIS, P_R is dissipated power at each relay transmit-receive antenna, here two sets of antennas are considered for half duplex AF relay, and N_{AF}, N_{RIS} is the number of antennas for AF relay and RIS.

It should be pointed out that energy efficiency is of great significance to a factory that its improvement can not only greatly reduce the energy cost, but also better respond to the call of the green factory and green communication.

Finally, in order to achieve the maximum energy efficiency under the lowest delay, that we mainly focus on the delay introduced by relay, here an effective energy efficiency η' can be defined as:

$$\eta' = \frac{C * \tau_{path}}{P_{all} * \tau} = \frac{C * \tau_{path}}{P_{all} * (\tau_{path} + \tau_{relay})} \quad \textbf{(23)}$$

Then, Q is defined as

$$Q = \frac{C * \tau_{path}}{P_{all} * (\tau_{path} + \omega * \tau_{relay})} \quad \textbf{(24)}$$

where ω represent the weight of delay.

Therefore, the optimization goals in the system with relay group $\mathcal{R}$ can be expressed as:

$$\underset{\mathcal{R}}{Maximize} \quad Q = \frac{C * \tau_{path}}{P_{all} * \omega * (\tau_{path} + \tau_{relay})} \quad \textbf{(25)}$$

$Subject$ to

$C.1$ $R(i) = \{0,1\}$ $i \in \mathcal{R}$

$C.2$ $\gamma > \gamma_{th}$

$C.3$ $\gamma_i > \gamma_{thi}$ $i \in \mathcal{R}, R(i) = 1$

$C.4$ $d(R_i - R_j) < A$ $i,j \in \mathcal{R}, R(i), R(j) = 1$

$C.5$ $\sum_i^{i\in\mathcal{R}} R(i) < \lambda$

$C.6$ $|\boldsymbol{f_S}s|^2 = 1$

$C.7$ $|\boldsymbol{f_R}y_{R_{AF}}|^2 = 1$

where C.1 denotes the relay state in $\mathcal{R}$. γ_{th}, γ_{th_i} are the SNR threshold at the user and relays respectively in C.2,3, which ensures that the signal can be received normally, especially after selecting several RISs. Where $d(R_i - R_j)$ represents the distance between R_i and R_j. The max serviceable distance of relay and max hop number in a selected relay link are limited to A and λ in C.4,5. The power constraints of beamforming for base station and AF relay are defined in C.6,7.

3 Joint Optimization Scheme

In the factory scenario, system delay and energy efficiency are critical issues for a network that need to be considered, especially gets more complicated with the introduction of RIS. Besides, the demands for system delay and energy efficiency are not the same in different scenarios. As for a multi-hop hybrid relay system, a relay is added to the selected relay link, system performance will not necessarily be better than ever, even lower. Therefore, during the relay selection, two hops, three hops, or even five hops all are possible to gain the best effect.

On account of the relay selection problem can be simplified into a real-time path optimization problem, that is, searching for the optimal solution in a complex and changeable environment. Besides, it is obviously a non-deterministic polynomial complete problem (NP-C) and the optimal solution of this problem can be obtained only by exhaustion.

Along with the number of relays under millimeter-wave communication increasing significantly, the solution space generated will expand rapidly at the same time, and exhaustive methods can no longer meet the demands. It is assumed that all channel status information (CSI) is perfectly known, then the solution space is all possible relay links, and the goal is to maximize the value Q.

3.1 SA-based Relay Selection Scheme

The original problem can be decomposed into an optimization process in a finite solution space and SA is a heuristic algorithm with low complexity. Hence, a multi-hop hybrid relay selection scheme based on the SA algorithm is developed. As algorithm 1 shows: we initialize the solution space S, T_{min}, δ, random v and obtain the value of Q (24) with a relay link $\mathcal{R}'$, which S contains all possible relay links $\mathcal{R}'$. Then based on the distance between the base station, user, and each relay in $\mathcal{R}'$, SNR of user and each relay, and P_{out} among base station, user and each relay in $\mathcal{R}'$to determine whether the communication is successful with the selected $\mathcal{R}'$ (C.2,3,4). If it fails, set the value of Q to 0.

Then, the new $\mathcal{R}'$ will be accepted if the next Q is greater than old one or on the basis of Metropolis rule as algorithm 2, which only the former will lower T through $T = T * log(1+\delta)$. Following, a new $\mathcal{R}'$ is generated with a v adjacent to the last accepted $\mathcal{R}'$ and the value of Q can be obtained with the new relay link $\mathcal{R}'$, which then will be determined whether to accept the new $\mathcal{R}'$. By repeatedly searching, finally, the best $\mathcal{R}'$ can be obtained when the probability of accepting a worse $\mathcal{R}'$ is too small and a better $\mathcal{R}'$ cannot be found for a long time that means the maximum number of cycles is exceeded.

Algorithm 1. SA-based relay selection

initialize: $S,\ T_{min},\ T,\ \delta$
Set v = random, $\mathcal{R}' = S(v)$, Get value Q
if $d(R_i, R_j) > A \quad \forall i, j \in \mathcal{R}'$ or $P_{out} = 1$ or $\gamma_i < \gamma_{thi} \quad \forall i \in \mathcal{R}'$ or $\gamma < \gamma_{th}$ **then**
    Set $Q = 0$
end if
Set $counter = 0$
while $T > T_{min}$ **do**
    Set $v_{new} = v + \Delta v$, Get value Q_{new}
    if $d(R_i, R_j) > A \quad \forall i, j \in \mathcal{R}'$ or $P_{out} = 1$ or $\gamma_i < \gamma_{thi} \quad \forall i \in \mathcal{R}'$ or $\gamma < \gamma_{th}$ **then**
        Set $Q = 0$
    else
        Get value $\Delta Q = Q_{new} - Q$
    end if
    if $\Delta Q > 0$ **then**
        Set $Q = Q_{new}, v = v_{new}, T = T * log(1+\delta)$
    else
        if Metropolis $(\Delta Q,\ T)$ **then**
            Set $Q = Q_{new}, v = v_{new}$
        end if
        Set $counter = counter + 1$
    end if
    if $counter > counter_{max}$ **then**
        Set $Q = Q_{new}, v = v_{new}$
        Break
    end if
end while

Algorithm 2. Metropolis $(\Delta Q,\ T)$

Set Q , T
if $e^{-\frac{\Delta Q}{T}} > rand(0,1)$ **then**
    Return 1
else
    Return 0
end if

Algorithm 3. Greedy-based relay selection

initialize: $\mathcal{R}'$
Set $t = 0,\ \rho(0) = 0$
while 1 **do**
for R in $\mathcal{R}$ **do**
    Add R to $\mathcal{R}'$
    Get value $Q(\mathcal{R}')$
    if $d(R_i, R_j) > A \quad \forall i, j \in \mathcal{R}'$ or $P_{out} = 1$ or $\gamma_i < \gamma_{thi} \quad \forall i \in \mathcal{R}'$ or $\gamma < \gamma_{th}$ **then**
        Set $Q = 0$
    end if
    Remove R from $\mathcal{R}'$
end for
$\rho(t) = max(\ Q(\mathcal{R}'))$
if $\rho(t) \le \rho(t-1)$ or $t \ge \lambda$ **then**
    Break
else
    $\mathcal{R}' = argmax(\ Q(\mathcal{R}'))$
    Remove $\mathcal{R}'$ from $\mathcal{R}$
    Set $t = t + 1$
end if
end while

3.2 Greedy-based Relay Selection Scheme

Here, by applying the idea of hierarchical search, a lower algorithm complexity is considered. Then, on the basis of greedy strategy, a hierarchical heuristic optimization is proposed and applied in multi-hop hybrid relay selection. As algorithm 3 shows: we initialize the selected relay link $\mathcal{R}'$ and set $t = 0, \rho(0) = 0$. Then, a relay is selected from $\mathcal{R}$ and added in $\mathcal{R}'$. Meanwhile, obtain the value of Q (24) with a relay link $\mathcal{R}'$ and based on the distance between base station, user and each relay in $\mathcal{R}'$, SNR of user and each relay, and P_{out} among base station, user, and each relay in $\mathcal{R}'$ to determine whether the communication is successful with $\mathcal{R}'$ (C.2,3,4), that if it fails, set the value of Q to 0. Then, remove the relay from $\mathcal{R}'$ and repeat until all relays are traversed in $\mathcal{R}$.

Following, the max Q is obtained with $\mathcal{R}'$, which means that the first hop of relay selection is over and then remove $\mathcal{R}'$ from $\mathcal{R}$, if the maximum number of hops is not reached (C.5) or the max Q is greater than the previous value. Then repeat it until the maximum number of hops is reached (C.5) or the max Q is not greater than the previous value and finally, the best $\mathcal{R}'$ can be obtained.

3.3 Complexity Analysis

Considering the worst case within the allowable error range, the solution space of the problem can be expressed as $S = \sum_{k=1}^{k=\lambda-1} A_n^k$, where n is the number of relays and λ is the number of hops. Let O(n) be the time required to calculate the system performance after relay selection. Therefore, the time complexity of the exhaustive algorithm can be expressed as O($n^{\lambda-1}$) * O(n), and the time complexity of the algorithm based on greedy strategy can be expressed as O((λ-1) * n) * O(n), because SA is a random algorithm and its time complexity is related to the required result accuracy, the time complexity of SA-based algorithm can be expressed as O(c) * O(n), where c is the maximum number of iterations set by SA algorithm. Generally, we set n << c << $n^{\lambda-1}$. Therefore, the complexity ranking of the three algorithms is: exhaustive algorithm >> SA based algorithm >> greedy-based algorithm.

4 Numerical Results

In this section, a communication system is investigated about the performance of different algorithms with the hybrid AF relay and RIS in Figure 1, which the maximum serviceable distance is both a circular area with radius of 20m.. The AF relay and RIS are assumed both randomly and uniformly placed in the 20m*20m*10m factory, where AF relay equipped with 16 antennas, user equipped with 4 and base station equipped with 64. Besides, the SNR reception threshold at the relay and user is set to 0 dBm and 10 dBm respectively. All presented illustrations have been averaged results over 100 independent relay's probability of outage and the channel realizations, and the confidence level we consider in this paper is 95%. All parameters are summarized in Table 1 according to [6, 16, 23].

Table 1. Simulation and algorithmic parameters

Parameters	Values	Parameters	Values
Outage probability constant ε:	0.5	Amplitude at each element of RIS η_i :	0.9
Background noise and receive noise N_0, N_1 :	-3dB	Dissipateed power at RIS and AF relay P_R:	10dBm
System delay caused by AF relay τ_{AF} :	50ns	System delay caused by RIS τ_{RIS}	1ns
Transmit power at base station P_S :	43dBm	Transmit power at AF relay P_r :	30dBm
Transmission data size δ :	1Kb	Circuit dissipated power coefficients ξ :	1.25
System delay weight in optimization w :	100	Maximum hops of communication λ :	5
Bandwidth W	200Mb	The number of channel rays L	4

In Figure 2, we investigated the system performance for the SNR of transmitting signal, assuming there are 5 AF relays and 10 RISs in the scene. Therein, the number of RIS elements is 64. In Figure 2(a), as SNR increased from 5 to 35(dB), Q increases first, then reduces gradually. It is evidently that when SNR is 17(dB), the maximum value is obtained. This is due to the fact that with the increase of transmission signal SNR, although the spectral efficiency of the signal also increases in Figure 2(c), the increased amplitude after passing through one or more relays is greatly diluted, resulting in the continuous reduction of the effective energy efficiency of the system. In addition, Figure 2(b) shows that the curve of energy efficiency is almost the same as Q value, which proves that the delay effect caused by AF relay can be almost ignored for the current communication conditions.

Furthermore, in Figure 2(d) as the SNR increases, system delay decreases until it converges to $4.8\mu s$, when the SNR is 24 dB. It can be explained by that when the SNR is large enough, more hops will lead to the introduction of additional delay, but it can still slightly improve the effective energy efficiency of the system, and finally make the system delay in the Figure 2(d) increase continuously under the condition of high SNR. This can be also well supported by the four hop and three hop curves in the Figure 2(d). Finally, an interesting result is shown that when the channel conditions are good, such as when the SNR is high, the performance of SA based method is close to exhaustive. When the channel conditions are poor, there is a certain gap between them. Therefore, it is necessary to measure the algorithm performance and algorithm complexity. But the greedy-based algorithm has a certain gap compared with SA-based algorithm as analyzed, especially when SNR is less than 30(dB).

Figure 3 shows the relationship between system performance and the RIS/relay density ratio with 20 total relays. Along with the increase of RIS/relay density ratio, there is a maximum value of Q at 80% in Figure 3(a). It can be illustrated perfectly by that RIS is a passive relay and although it can improve the system energy efficiency, without the assistance of AF relay, RIS is difficult to ensure that the communication signal strength can reach the threshold. In addition, it is evidently in the Figure 3(b) that the energy efficiency of the network with only AF relay is about 15% less than the network with only RIS, and the energy efficiency of the AF and RIS hybrid relay network is almost the same as the network with only RIS, which the advantages of the proposed active and passive relay hybrid network is proved well. Finally, in Figure 3(c) the spectral efficiency reaches maximum when the RIS/relay density ratio is 90%, and most of the results of four-hops and five-hops are higher than those of three-hops, which shows that the increase of hop number can not only enhance the coverage area of communication, but also improve a certain spectral efficiency.

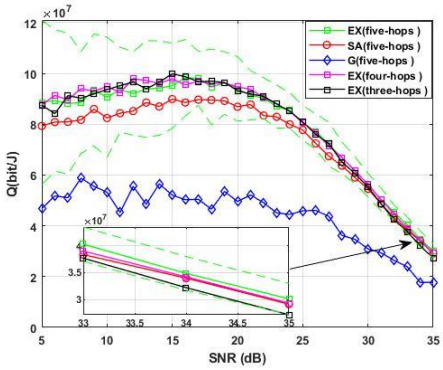

(a) Q versus SNR of transmitting signal

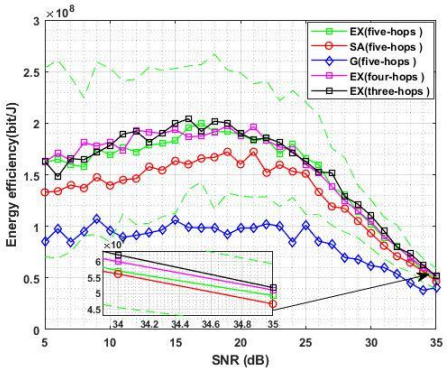

(b) Energy efficiency versus SNR of transmitting signal

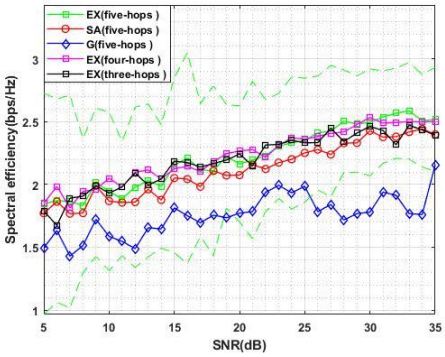

(c) Spectral efficiency versus SNR of transmitting signal

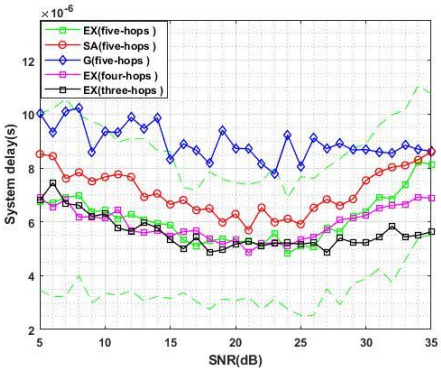

(d) System delay versus SNR of transmitting signal

Figure 2. System performance versus SNR of transmitting signal with 15 relays including 5 AF relays and 10 RISs, where the number of elements of RIS is 64 and the number of antennas of AF relay is 16. The dotted line in the figure represents the confidence interval of the corresponding data

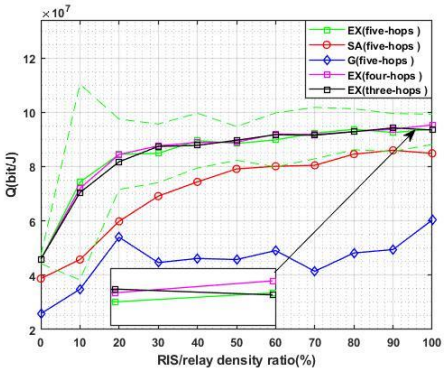

(a) Q versus RIS/relay density ratio (%)

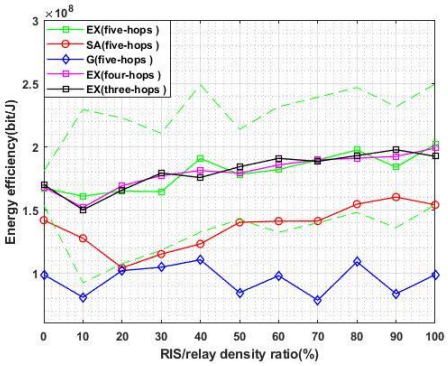

(b) Energy efficiency versus RIS/relay density ratio (%)

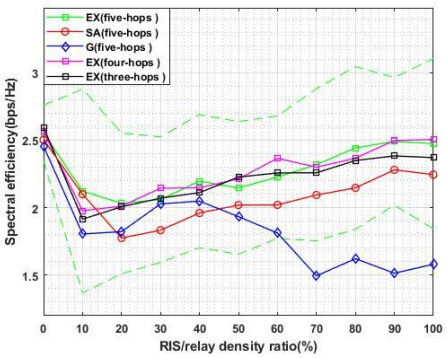

(c) Spectral efficiency versus RIS/relay density ratio (%)

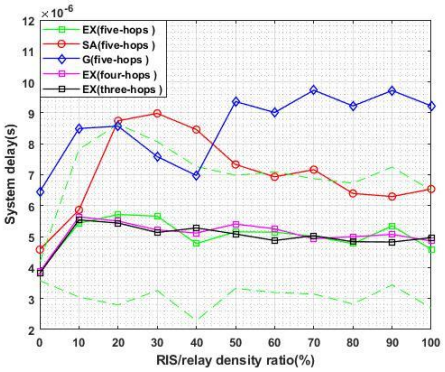

(d) System delay versus RIS/relay density ratio (%)

Figure 3. System performance versus RIS/relay density ratio (%) with 20 relays, where the number of elements of RIS is 64, the number of antennas of AF relay is 16 and SNR of transmitting signal is 22dB. The dotted line in the figure represents the confidence interval of the corresponding data

When the RIS/relay density ratio is small, the spectral efficiency with greedy-based scheme is about 85% of exhaustion. However, when the RIS/relay density ratio increases to more than 70%, the gap expands rapidly, which can be explained by that the solution space becomes sparse and it pays less attention to long-term benefits. Besides, Figure 3(d) shows that the lowest system delay is reached at 0% ratio and the value with full of RIS is about 118% of that without RIS, which illustrates that the network full of RIS cannot improve the system delay. The last but not least, more attention is paid to the delay introduced by the relay in the paper and the optimization goal is to give the relay the effective energy efficiency with large weight. Therefore, the joint optimization results with low delay and high energy efficiency are produced, and the numerical results also show the effectiveness of the proposed model.

Figure 4 displays system performance with respect to the number of RIS elements with 5 AF relays and 10 RISs. As it is depicted in Figure 4(a) that along with the number of RIS elements increased from 16 to 256, the corresponding value of Q decreased by about 62% due to the dissipated power in each element, but it is still higher than the result without RIS. Moreover, we can find that the energy efficiency of the system with RISs in the network is higher than that without RISs when the number of RIS elements is less than 128 in Figure 4(b). However, with the increase of the number of RIS components, the gap is shrinking, and it is surpassed when the number of RIS components is 128. It perfectly illustrates that with the increase of the number of components, RIS not only provides huge gain, but also reduces the energy efficiency due to the dissipated power in each element. In addition, Figure 4(c) depicts that with the increase of the number of components, the spectral efficiency with RIS increases rapidly, and gradually approaches the result without RIS. This result shows that increasing the number of elements can indeed significantly improve the signal gain of RIS, but considering the energy loss generated by each element, we need to choose the spectral efficiency and energy efficiency according to different needs.

Finally, in Figure 4(d) along with the increasing number of RIS components, the system delay decreases gradually, which is close to the result without RIS. It is obvious that the system delay of 10RISs is lower than that of 15RISs, which further reflects the advantages of hybrid relay system. The last but not least, with the increase of the number of RIS elements, the cost up at the same time. Therefore, it is a challenge to obtain an optimal number of RIS components for the large-scale application of RIS in the future.

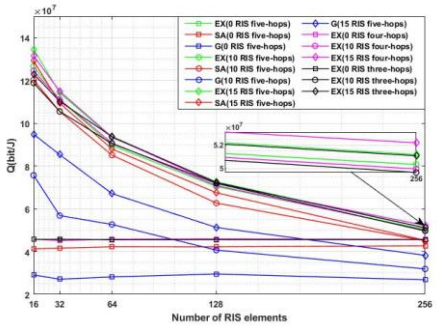

(a) Q versus number of RIS elements

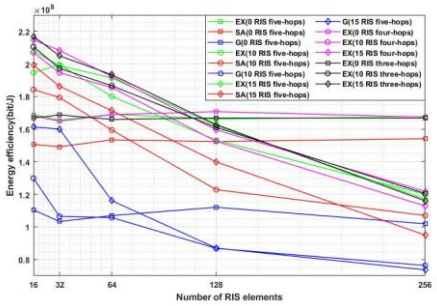

(b) Energy efficiency versus number of RIS elements

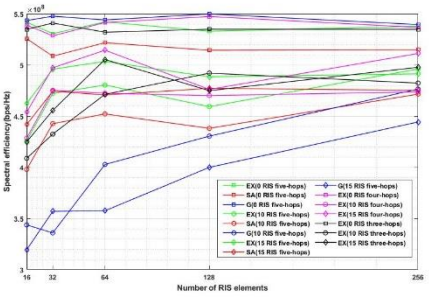

(c) Spectral efficiency versus number of RIS elements

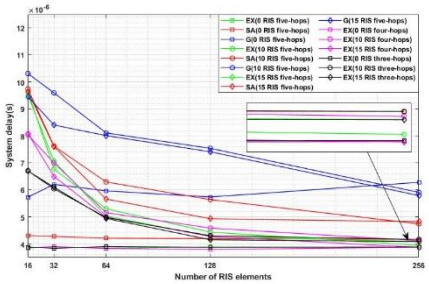

(d) System delay versus number of RIS elements

Figure 4. System performance versus the number of RIS elements with 15 relays including 0,10,15 RISs separately, where the number of antennas of AF relay is 16 and the SNR of transmitting signal is 22dB. The dotted line in the figure represents the confidence interval of the corresponding data

5 Conclusion

The performance of multi-hop hybrid active–and-passive relay selection in mmWave communication is investigated in this paper, and based on SA algorithm, an effective energy efficiency model is proposed to consider the joint optimization of delay and energy efficiency. Moreover, a hierarchical heuristic optimization algorithm with lower complexity is proposed. In addition, the influence of RIS/AF relay density ratio, SNR of the transmitted signal, and the number of RIS elements are also evaluated.

Numerical results show that the provided SA-based algorithm performs almost as well as the exhaustion in good communication condition, which owns the lower complexity, and a hierarchical heuristic optimization algorithm with lower complexity is investigated and proved to be feasible comparing with other algorithms. Meanwhile, it is shown that

the proposed effective energy efficiency reflects the balance between system energy efficiency and system delay very well. Moreover, it is obvious that the number of RIS elements have a significant positive correlation with the spectral efficiency, and there is an optimal value for the proportion of RIS/AF relays and the SNR of the transmitted signal. Therefore, it is necessary to determine an optimal active and passive relay network deployment in the future. Finally, deploying passive relays to an active relay network for signal transmission can greatly improve the energy efficiency of the system and reduce deployment costs and transmission delays at the expense of a small amount of system capacity and a more complex relay system. Then, a novel hybrid relay network in mmWave communication is unveiled in this paper, which provides a promising alternative architecture for mmWave even terahertz communication in the future. Last but not least, the impact of hops is not well reflected due to the limitation of scene size. Hence, a more complex models and scenarios with multiple users and consideration of interference between relays and users will be considered in the future work.

6 Acknowledgments

The work was supported in part by National Natural Science Foundation of China (Grant number 61871339, 62171392), in part by the Natural Science Foundation of Fujian Province of China No. 2021J01004.

References

[1] A. Z. Yalcın, Y. Yapıcı, Multiuser precoding for sum-rate maximization in relay-aided mmwave communications, *IEEE Transactions on Vehicular Technology*, Vol. 69, No. 6, pp. 6808-6812, June, 2020.

[2] Q. Hu, D. M. Blough, Relay Selection and Scheduling for Millimeter Wave Backhaul in Urban Environments, *2017 IEEE 14th International Conference on Mobile Ad Hoc and Sensor Systems (MASS)*, Orlando, FL, USA, 2017, pp. 206-214.

[3] S. H. Kim, T. V. K. Chaitanya, T. Le-Ngoc, J. Kim, Rate maximization based power allocation and relay selection with iri consideration for two-path af relaying, *IEEE Transactions on Wireless Communications*, Vol. 14, No. 11, pp. 6012-6027, November, 2015.

[4] N. Wei, X. Lin, Z. Zhang, Optimal relay probing in millimeter-wave cellular systems with device-to-device relaying, *IEEE Transactions on Vehicular Technology*, Vol. 65, No. 12, pp. 10218-10222, December, 2016.

[5] S. Atapattu, N. Ross, Y. Jing, Y. He, J. S. Evans, Physical-layer security in full-duplex multi-hop multi-user wireless network with relay selection, *IEEE Transactions on Wireless Communications*, Vol. 18, No. 2, pp. 1216-1232, February, 2019.

[6] Z. Li, L. Xiang, X. Ge, G. Mao, H. C. Chao, Latency and reliability of mmwave multi-hop v2v communications under relay selections, *IEEE Transactions on Vehicular Technology*, Vol. 69, No. 9, pp. 9807-9821, September, 2020.

[7] G. Davis, 2020: Life with 50 billion connected devices, *2018 IEEE International Conference on Consumer Electronics (ICCE)*, Las Vegas, NV, USA, 2018, pp. 1-1.

[8] T. S. Rappaport, S. Sun, R. Mayzus, H. Zhao, Y. Azar, K. Wang, G. N. Wong, J. K. Schulz, M. Samimi, F. Gutierrez, Millimeter wave mobile communications for 5g cellular: It will work!, *IEEE Access*, Vol. 1, pp. 335-349, May, 2013.

[9] G. C. Alexandropoulos, P. Ferrand, J. Gorce, C. B. Papadias, Advanced coordinated beamforming for the downlink of future lte cellular networks, *IEEE Communications Magazine*, Vol. 54, No. 7, pp. 54-60, July, 2016.

[10] J. Zuo, J. Zhang, C. Yuen, W. Jiang, W. Luo, Energy-efficient downlink transmission for multicell massive das with pilot contamination, *IEEE Transactions on Vehicular Technology*, Vol. 66, No. 2, pp. 1209-1221, February, 2017.

[11] C. Huang, A. Zappone, M. Debbah, C. Yuen, Achievable Rate Maximization by Passive Intelligent Mirrors, *2018 IEEE International Conference on Acoustics, Speech and Signal Processing (ICASSP)*, Calgary, AB, Canada, 2018, pp. 3714-3718.

[12] T. N. Do, D. B. da Costa, T. Q. Duong, B. An, Improving the performance of cell-edge users in miso-noma systems using tas and swipt-based cooperative transmissions, *IEEE Transactions on Green Communications and Networking*, Vol. 2, No. 1, pp. 49-62, March, 2018.

[13] T. D. Hieu, T. T. Duy, B. Kim, Performance enhancement for multihop harvest-to-transmit wsns with path-selection methods in presence of eavesdroppers and hardware noises, *IEEE Sensors Journal*, Vol. 18, No. 12, pp. 5173-5186, June, 2018.

[14] Q. Wu, R. Zhang, Intelligent reflecting surface enhanced wireless network via joint active and passive beamforming, *IEEE Transactions on Wireless Communications*, Vol. 18, No. 11, pp. 5394-5409, November, 2019.

[15] L. Zhang, X. Q. Chen, S. Liu, Q. Zhang, J. Zhao, J. Y. Dai, G. D. Bai, X. Wan, Q. Cheng, G. Castaldi, V. Galdi, T. J. Cui, Space-time-coding digital metasurfaces, *2019 Thirteenth International Congress on Artificial Materials for Novel Wave Phenomena (Metamaterials)*, Rome, Italy, 2019, pp. X-128-X-130.

[16] C. Huang, A. Zappone, G. C. Alexandropoulos, M. Debbah, C. Yuen, Reconfigurable intelligent surfaces for energy efficiency in wireless communication, *IEEE Transactions on Wireless Communications*, Vol. 18, No. 8, pp. 4157-4170, August, 2019.

[17] Q. Wu, S. Zhang, B. Zheng, C. You, R. Zhang, Intelligent Reflecting Surface-Aided Wireless Communications: A Tutorial, *IEEE Transactions on Communications*, Vol. 69, No. 5, pp. 3313-3351, May, 2021.

[18] S. Abeywickrama, R. Zhang, Q. Wu, C. Yuen, Intelligent reflecting surface: Practical phase shift model and beamforming optimization, *IEEE Transactions on Communications*, Vol. 68, No. 9, pp. 5849-5863, September, 2020.

[19] P. Xu, G. Chen, Z. Yang, M. D. Renzo, Reconfigurable intelligent surfaces-assisted communications with discrete phase shifts: How many quantization levels are required to achieve full diversity?, *IEEE Wireless Communications Letters*, Vol. 10, No. 2, pp. 358-362, February, 2021.

[20] C. Huang, G. Chen, Y. Gong, M. Wen, J. A. Chambers, Deep reinforcement learning-based relay selection in intelligent reflecting surface assisted cooperative networks, *IEEE Wireless Communications Letters*, Vol. 10, No. 5, pp. 1036-1040, May, 2021.
[21] E. Björnson, Ö. Özdogan, E. G. Larsson, Intelligent Reflecting Surface Versus Decode-and-Forward: How Large Surfaces are Needed to Beat Relaying?, *IEEE Wireless Communications Letters*, Vol. 9, No. 2, pp. 244-248, February, 2020.
[22] M. D. Renzo, K. Ntontin, J. Song, F. H. Danufane, X. Qian, F. Lazarakis, J. D. Rosny, D.-T. Phan-Huy, O. Simeone, R. Zhang, M. Debbah, G. Lerosey, M. Fink, S. Tretyakov, S. Shamai, Reconfigurable Intelligent Surfaces vs. Relaying: Differences, Similarities, and Performance Comparison, *IEEE Open Journal of the Communications Society*, Vol. 1, pp. 798-807, June, 2020.
[23] Z. Abdullah, G. Chen, S. Lambotharan, J. A. Chambers, A hybrid relay and intelligent reflecting surface network and its ergodic performance analysis, *IEEE Wireless Communications Letters*, Vol. 9, No. 10, pp. 1653-1657, October, 2020.
[24] J. Lyu, R. Zhang, Hybrid Active/Passive Wireless Network Aided by Intelligent Reflecting Surface: System Modeling and Performance Analysis, *IEEE Transactions on Wireless Communications*, Vol. 20, No. 11, pp. 7196-7212, November, 2021.
[25] Y. Hei, S. Yu, C. Liu, W. Li, J. Yang, Energy-efficient hybrid precoding for mmwave mimo systems with phase modulation array, *IEEE Transactions on Green Communications and Networking*, Vol. 4, No. 3, pp. 678-688, September, 2020.
[26] C. Chen, C. Tsai, Y. Liu, W. Hung, A. Wu, Compressive sensing (cs) assisted low-complexity beamspace hybrid precoding for millimeter-wave mimo systems, *IEEE Transactions on Signal Processing*, Vol. 65, No. 6, pp. 1412-1424, March, 2017.
[27] J. Jin, Y. R. Zheng, W. Chen, C. Xiao, Hybrid precoding for millimeter wave mimo systems: A matrix factorization approach, *IEEE Transactions on Wireless Communications*, Vol. 17, No. 5, pp. 3327-3339, May, 2018.
[28] A. Alkhateeb, O. El Ayach, G. Leus, R. W. Heath, Channel estimation and hybrid precoding for millimeter wave cellular systems, *IEEE Journal of Selected Topics in Signal Processing*, Vol. 8, No. 5, pp. 831-846, October, 2014.

Biographies

Zejing Yang received his B.S. degree from Xiamen University, Xiamen, China in 2019. He is currently pursuing the M.S. degree in electronic communication engineering with Xiamen University. His research interests include MmWave Communication and wireless network with intelligent reconfigurable surface.

Jianzheng Wang received his B.S. degree in Communication Engineering in 2018 from Xiamen University, Xiamen, China, where He is currently pursuing the M.S. degree. His current research interests include MmWave communication and Machine learning applied in wireless communication.

Yifeng Zhao received his B.S. degree in Communication Engineering in 2002, M.S degree in Electronic Circuit System in 2005 and Ph.D. degree in Communication Engineering in 2014 from Xiamen University. He is an assistant professor of Communication Engineering, Xiamen University, Xiamen, Fujian, China. His current research interests include Mmwave communication, Massive MIMO and Machine learning applied in wireless communication.

Lianfen Huang received her B.S. degree in Radio Physics in 1984 and PhD in Communication Engineering in 2008 from Xiamen University. She was a visiting scholar in Tsinghua University in 1997. She is a professor in the Department of Communication Engineering, Xiamen University, Xiamen, Fujian, China. Her current research interests include wireless communication, wireless network and signal process.

Zhiyuan Shi received his B.S. degree in radio physics in 1984, M.S. degree in radio electronics in 1991 from Xiamen University. He is a Professor in the Department of electronic engineering, Xiamen University, Xiamen, Fujian, China. His current research interests include wireless communication, circuit and system.